Planetary and Space Science 96 (2014) 125–132

Contents lists available at ScienceDirect

Planetary and Space Science

journal homepage: www.elsevier.com/locate/pss

Magnetic pileup boundary and field draping at Comet Halley

M. Delva [a,*], C. Bertucci [b], K. Schwingenschuh [a], M. Volwerk [a], N. Romanelli [b]

[a] Space Research Institute, Austrian Academy of Sciences, Graz, Austria
[b] Astrophysical Plasmas, IAFE, Buenos Aires, Argentina

ARTICLE INFO

Article history:
Received 6 November 2013
Received in revised form
11 February 2014
Accepted 16 February 2014
Available online 2 March 2014

Keywords:
Comets
Solar wind interaction
Induced magnetosphere
Plasma boundaries
Magnetic field draping

ABSTRACT

The approach of the Rosetta S/C to Comet Churyumov–Gerasimenko in 2014 reactivates the interest in the plasma interaction of the solar wind with the cometary coma. In preparation for the upcoming S/C observations and the start of outgassing of the cometary nucleus, we reinvestigate the magnetic field data from the Vega-1 S/C at the flyby of Comet Halley (1986), in search of the magnetic pileup boundary and increase of field line draping. The magnetic pileup boundary has been identified as a common feature for unmagnetized bodies with an induced magnetosphere. This boundary marks the outer edge of the magnetic pileup region, also known as the magnetic barrier region, in which the magnetic field is strong and highly draped. Initially, the magnetic field draping around Comet Halley was clearly identified from the Vega-1 magnetometer data through reversal of the field component in direction to the Sun at closest approach.

Here, a detailed analysis is performed in regions further upstream in the magnetosheath. The Vega-1 high resolution magnetometer data on the in- and outbound leg but inside the bow wave are reinvestigated in search for the magnetic pileup boundary as an indicator for the outer edge of the magnetic barrier. The magnetic field pileup region is studied using the correlation between the field component towards the Sun and the radial component in an aberrated cometocentric frame; this technique proved very successful for Mars and also for comets Giacobini–Zinner and Halley in the case of Giotto observations. We can clearly identify the different regimes in the magnetic field data, on the in- and outbound leg of the orbit. Waves just within the newly determined magnetic pileup region have properties different from mirror mode waves, whereas waves observed out of the magnetic pileup boundary are confirmed as mirror mode. The boundaries found at Comet Halley prove that also the detailed structure of the interaction of unmagnetized bodies with an atmosphere with the solar wind is valid for active comets, but with larger space scale.

1. Introduction

New interest goes to the interaction of the solar wind with comets, as the approach of the Rosetta spacecraft (S/C) to Comet Churyumov–Gerasimenko will occur in the near future (May 2014) (Glassmeier et al., 2007a). The S/C carries a magnetometer on the orbiter (Glassmeier et al., 2007b) as well as on the lander (Auster et al., 2007). Both sensors are designed to reveal details of the evolution of the different plasma boundaries and regimes during the development of the cometary coma when approaching the Sun.

From earlier missions to comets, e.g. Vega-1 and -2 to Comet Halley, Giotto to Comet Halley and Grigg–Skjellerup (von Rosenvinge et al., 1986) and ICE to Comet Giacobini–Zinner (Reinhard, 1986), magnetometer measurements proved the general picture of draping of the interplanetary magnetic field lines around the obstacle, formed by the cometary coma (Alfvèn, 1957).

Since the time of these cometary missions, the solar wind interaction with unmagnetized planets with an atmosphere was studied in great detail and specific regions with different characteristics in the magnetic field and/or the plasma composition have been identified. An extensive review of the different regions of the induced magnetospheric interaction is found in Bertucci et al. (2011). Inside the bow shock, the magnetosheath field shows strong wave activity and turbulence up to a region, where the wave activity disappears abruptly; this is called the magnetic pile-up boundary (MPB). The MPB is the outer limit of the induced magnetosphere, and is also a plasma composition boundary, where the solar wind proton density drops sharply, the electron fluxes in the high-energy range decrease significantly and the planetary ion density starts to increase. Inside the MPB and especially on the dayside, field line draping starts and the field strength increases strongly over a small distance to a maximum value; this is the magnetic pileup region (MPR) in which the planetary ions dominate. Observation of a drop of the field strength at closest approach of a S/C to the planet indicates that the magnetic "cavity" boundary has been crossed, i.e. the S/C

* Corresponding author. Tel.: +43 316 4120 553; fax: +43 316 4120 590.
E-mail address: magda.delva@oeaw.ac.at (M. Delva).

http://dx.doi.org/10.1016/j.pss.2014.02.010
0032-0633

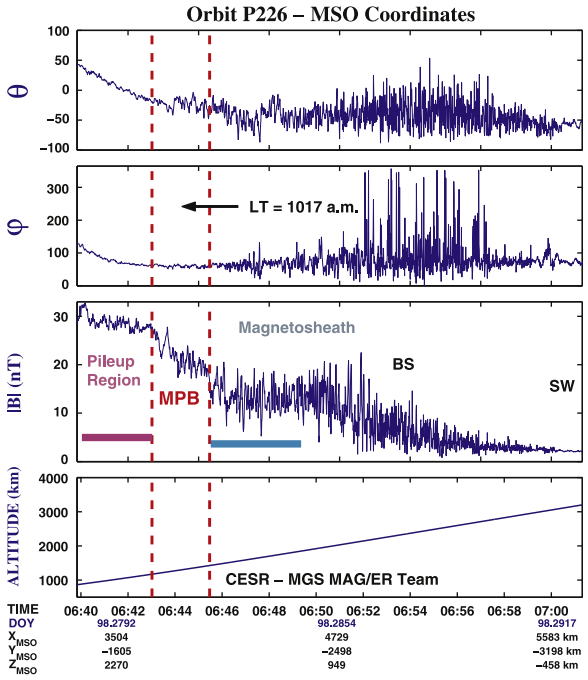

Fig. 1. Example of the magnetic pileup boundary and pileup region at Mars, from MGS data. The three upper panels show the magnetic field in spherical MSO coordinates and the magnetic field strength, the fourth panel displays the altitude above the planet. In panel three, the pink bar indicates the time interval with strong correlation between Bx_{IMF} and B_{rad}; for the interval marked with blue–green bar, the correlation is not existent (from Bertucci et al., 2003a). (For interpretation of the references to color in this figure legend, the reader is referred to the web version of this article.)

enters a region void of solar wind magnetic field; this is not always the case and depends mainly on the orbit of the S/C. Fig. 1 shows these different regions in the magnetic field observations at Mars from Mars Global Surveyor (MGS) (Bertucci et al., 2003a).

Attempts were made to identify the plasma boundaries sufficiently from magnetometer data only. At Comet Halley, the MPB was first identified from the Giotto magnetic field data as a sharp increase in the magnetic field strength (Neubauer, 1987). In a further step, a correlation technique was applied to these data to identify regions with explicit draping; the MPB separates the cometary magnetosheath, where there is no evidence of draping, from the magnetic pileup region where the field lines are strongly draped (Israelevich et al., 1994). The technique also allows to identify the MPB, when the signature in the magnetic field strength is ambiguous, as was the case for the Vega-1 and Vega-2 magnetometer data at Comet Halley. To detect the draping, a specific decomposition of the magnetic field vector is required. First, an aberration correction for the solar wind velocity as seen by the comet is performed: this implies a rotation, such that in the aberrated frame the x'-axis is anti-parallel to the onstreaming solar wind velocity as seen by the comet. Then, an electromagnetic reference frame (x_{IMF}, y_{IMF}, z_{IMF}) is defined, where the x_{IMF}-axis is equal to the x'-axis, the y_{IMF}-axis is defined by $-\boldsymbol{V}_{SW}\times\boldsymbol{B}_{IMF}$ and z_{IMF} completes the right hand system; now the magnetic field $\boldsymbol{B}_{IMF}$ is in the (x_{IMF}, z_{IMF})-plane. On this plane, the field vector is described by the component Bx_{IMF} (x_{IMF}-axis is anti-parallel to $\boldsymbol{V}_{SW}$) and the transverse component $Btrans_{IMF}$. The transverse component, in turn, can be decomposed in a radial part, B_{rad}, and a tangential part B_{tan} (Fig. 2, after Bertucci et al., 2003a). With this decomposition of the field vector, a draped field configuration around the obstacle at the origin of the reference frame will be revealed by the correlation between Bx_{IMF} and B_{rad}, along the S/C trajectory such that a decrease in the value of Bx_{IMF} leads to an

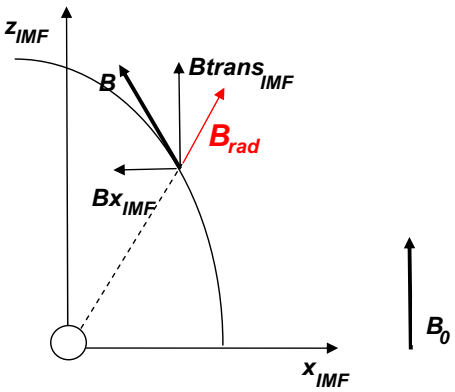

Fig. 2. Draping geometry in the (x_{IMF}, z_{IMF})-plane of the electromagnetic reference frame (x_{IMF}, y_{IMF}, z_{IMF}). $\boldsymbol{B}_0$ denotes an undraped field direction in the solar wind; $\boldsymbol{B}$ is the draped field with components Bx_{IMF}, $Btrans_{IMF}$ where $Btrans_{IMF}$ is decomposed in B_{rad} and B_{tan} (not shown).

increase of B_{rad} and vice versa; this is independent of the quadrant of the vectors (Israelevich et al., 1994).

In simple words: if the Bx_{IMF} component increases in value and the field becomes more parallel to the solar wind speed direction, the radial component B_{rad} will decrease. This is valid as long as there are no discontinuities or strong fluctuations in the solar wind in the analyzed time interval. The technique was applied to MGS data (Bertucci et al., 2003a) and Pioneer Venus Orbiter data (Bertucci et al., 2003b) to identify the MPB around Mars and Venus, respectively.

From the Soviet missions Vega-1 and -2 to Comet Halley, high resolution magnetic field data are still available; here, a detailed analysis of the field draping with the correlation technique is performed to reveal the extent of the induced magnetosphere within the bow wave.

The Vega-1 and -2 S/C flew by Comet Halley on 6 (9) March 1986, with closest approach at 8890 and 8030 km, respectively. From the plasma and magnetometer data, main new insights about the nature of the interaction of the solar wind with the non-magnetised cometary body were gained. The inbound bow wave was observed at a distance of 1.1×10^6 km from the nucleus. Draping was seen as an effect of two different interplanetary magnetic field (IMF) orientations hung up around the comet. On the inbound leg of the S/C trajectory to closest approach, the field component parallel to the solar wind velocity changed sign, due to the crossing of an IMF sector boundary. On the outbound trajectory, that field component showed the field reversal in timely reversed order. The field at the closest approach was interpreted as "old field" draped around the obstacle, with IMF direction opposite to that of the outer draped field layer (Riedler et al., 1986). The MPB could not be derived from the magnetometer data, since no sudden increase of the magnetic field strength was observed (Schwingenschuh et al., 1986).

In the earliest papers, a sharp increase in water group ion density and decrease in proton density at $\sim1.6\times10^5$ km from the nucleus in the Vega-2 plasma data led to the interpretation of a “cometopause” (Gringauz et al., 1986). Later analysis of multi-sensor data and comparison with the Giotto S/C observations indicated, that the sharp change in the Vega-2 plasma observations might be an observational effect; only the MPB, well identified in the Giotto magnetometer data at a closer distance to the nucleus (Neubauer, 1987), was interpreted as a real boundary (Rème et al., 1994).

2. Data analysis

In this paper, the Vega-1 high-resolution (10 vectors/s) magnetometer data between the inbound bow wave crossing (at 03:10 on Mar 06, 1986) and closest approach (07:20) are reinvestigated

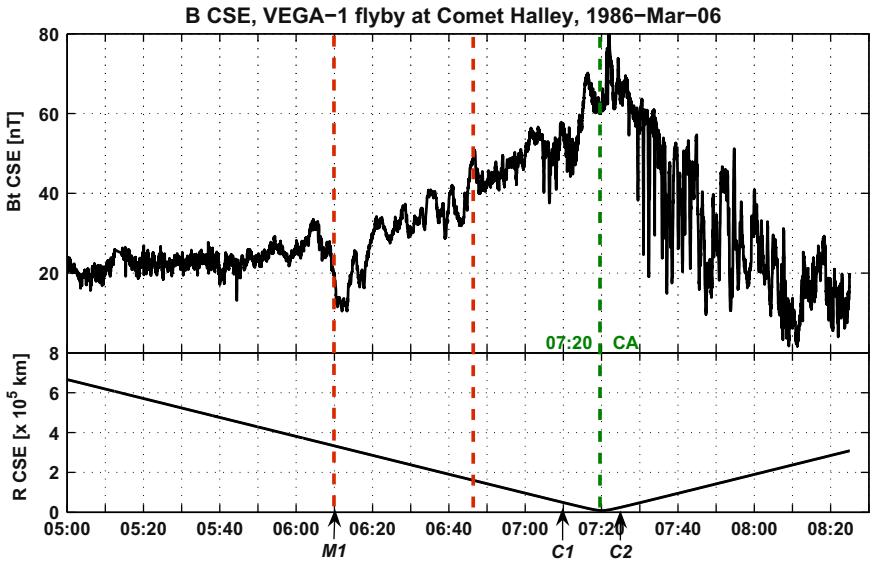

Fig. 3. Top panel: time series of high resolution magnetic field strength *Bt* in the magnetosheath around closest approach (CA, green bar at 07:20); fluctuations are significantly lower between 06:10 and 06:47, marked with red bars. Earlier detected features, marked as *M1*, *C1* and *C2*, are explained in the text. Lower panel: distance of the S/C to the comet. (For interpretation of the references to color in this figure legend, the reader is referred to the web version of this article.)

with the correlation technique (Israelevich et al., 1994; Bertucci et al., 2003a) in search for the MPB. The magnetometer data are given in the cometocentric reference frame CSE, which has its x_{CSE}-axis in direction to the Sun, y_{CSE}-axis opposite to the S/C velocity in the ecliptic plane and z_{CSE} positive to ecliptic North. A time series of the observed magnetic field strength for several hours (05:00 to 08:25) within the magnetosheath is shown in Fig. 3 in the CSE frame (bow wave crossing was at 03:10, closest approach at 07:20, dashed green line). A high level of variability occurs within the magnetosheath until 06:10 (first dashed red line), but later on, the fluctuation is weaker (until 06:47, second dashed red line, see also Schwingenschuh et al., 1986). Fig. 4 shows the projection of the (averaged) field vectors on the (x_{CSE}, y_{CSE})-plane for a full hour around closest approach.

Several boundaries were identified using the magnetometer data and the plasma data. A change in the slope of the magnetic field strength at 06:10 (distance 3.5×10^5 km) was identified as a quasi-stationary feature of Halley's inner coma, the so-called '*M1*' boundary or layer (Schwingenschuh et al., 1986). This coincides with the strong reduction of the variability, as seen in Fig. 3. At about the same distance, the solar wind population number density became comparable to that of the cometary implanted ions (Gringauz et al., 1986). The reported boundary was explained by a sudden change in the solar wind velocity, thus causing a different piling up of the interplanetary magnetic field lines. The *M1* boundary is located at approximately the same distance as the MPB reported from the Giotto S/C by Neubauer et al. (1986) where similar features were observed (except the gradual pileup), supporting the idea that *M1* is stationary and that *M1* might be the MPB. Furthermore, two boundaries *C1* (07:10, before closest approach) and *C2* (07:24 after closest approach) were identified from a change in the Bx_{CSE} component (Riedler et al., 1986). These boundaries separate regions with different draping pattern from a remnant magnetic field from a polarity change 8 h before the encounter. The changes in sign in Bx_{CSE} before and after closest approach *C1* and *C2* are clearly seen in the projected vectors of Fig. 4; see Fig. 7 for $\boldsymbol{B}$ in CSE components.

In terms of the MPB and MPR, the MPB starts at the time of reduction of the turbulence (06:10); after that, the start of the MPR is not obvious because the magnetic field strength increase is gradual and not extremely steep.

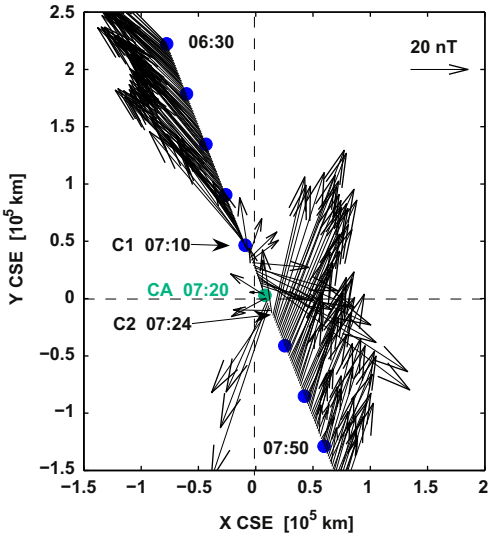

Fig. 4. Projection of the (averaged to 1 vector per 30 s; marks every 10 min) field vectors on the (x_{CSE}, y_{CSE})-plane for approximately 1 h around closest approach. The S/C approached the comet from the dusk side at large solar zenith angle. A change of sign in the Bx_{CSE} component at *C1* and *C2* is clearly seen.

A detailed analysis of sub-intervals with the correlation technique is expected to reveal more fine structure of the field in this region. This requires several transformations of the data, as described in the introduction. The aberration correction for the solar wind velocity as seen by the comet implies a rotation over $\sim 5^\circ$ around the z_{CSE}-axis, such that in the aberrated frame (x', y', z') the x'-axis is anti-parallel to the onstreaming solar wind velocity as seen by the comet. In a further step, the magnetic field vectors are decomposed according to the described technique and the Bx_{IMF} and the radial component B_{rad} are obtained.

2.1. Time-interval 06:00–07:00 before closest approach

The time interval 1986 Mar 06, 06:00–07:00 is divided into smaller intervals, to take the different features already reported in earlier analyses into account. Fig. 5 shows the field components in

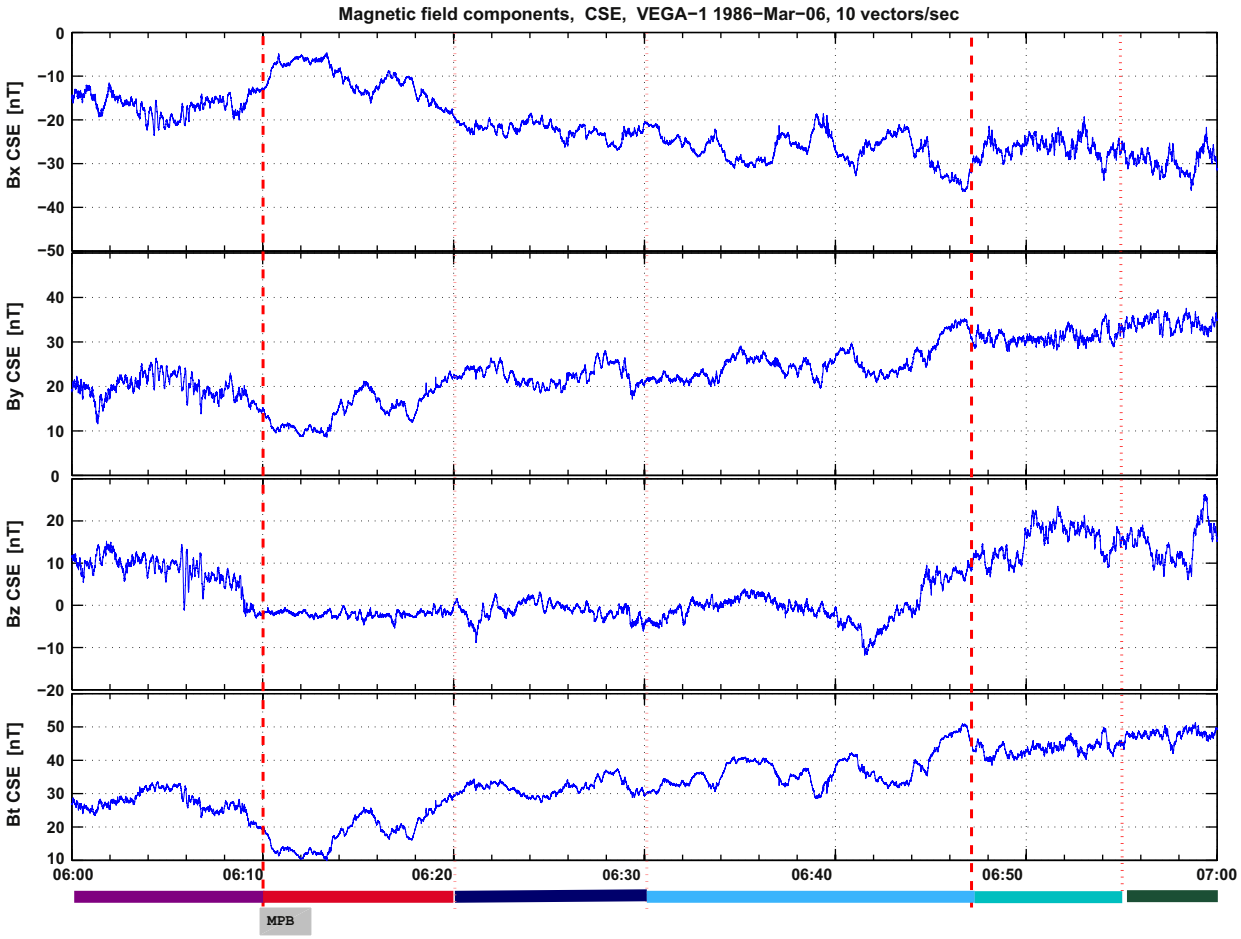

Fig. 5. Magnetic field components and total field in the CSE reference frame, 1986 Mar 06, 06:00–07:00 before closest approach (07:20); each time interval is indicated with a specific color. Variability is weaker between the vertical red dashed lines (06:10 to 06:47). The grey bar indicates the possible location of the inbound MPB according to the draping analysis. (For interpretation of the references to color in this figure legend, the reader is referred to the web version of this article.)

the CSE reference frame and the partition into sub-intervals. Fig. 6 displays the calculated correlation between the Bx_{IMF}- and B_{rad}-field components for each sub-interval.

We first examine the difference between the turbulent data part (06:00 to 06:10) and the data within the quiet interval (06:10 to 06:47); it should be noted that a rotation of the field vector occurs at 06:10. In the turbulent interval, correlation between Bx_{IMF} and B_{rad} field components is poor (Fig. 6, top left). Analysis of the subsequent intervals shows that only in some intervals an increase of the correlation occurs, i.e. draping is also not explicit in the range with low turbulence (Fig. 6, top right and middle). The interval 06:47 to 07:00 is divided at 06:55, because it was reported that at this time a cold slow ion plasma was entered; this region (S/C at distance of 1.2×10^5 km) was interpreted as the outer limit of the obstacle where the cometary ions dominate (Gringauz et al., 1986). However, the correlation analysis shows only similar low correlation in both parts (06:47 to 06:55, and 06:55 to 07:00, Fig. 6, lower panels).

Although the occurrence of fluctuations in the full hour of data is significantly reduced between 06:10 and 06:47, no significant difference is seen in the correlation from the more variable before 06:10 and the more quiet intervals after; also the reported boundary at 06:55 does not show up as a change in draping.

This means that from magnetic field point of view, the outer edge of the region with low turbulence, passed at 06:10, may be attributed to the MPB. Significant draping does not yet start and the magnetic field strength increases gradually by +35 nT over a large distance (from 3.5×10^5 km at 06:10 to 9.6×10^4 km at 07:00). At the time of the Giotto encounter, the situation was very different; a very sharp increase of +20 nT at a distance of 1.35×10^5 km was reported (Neubauer, 1987).

2.2. Time-interval 07:00 to 07:35 around closest approach (07:20)

We now analyze the time interval 1986 Mar 06, 07:00–07:35 around the closest approach. The data are divided into intervals, taking into account the tangential discontinuities *C1* at 07:10 before, resp. *C2* at 07:24 after closest approach (Fig. 7); these were interpreted as 'old' field reversals in the onstreaming SW, still draped around the comet (Riedler et al., 1986).

Fig. 8 shows the calculated correlation for the respective sub-intervals. For the time around closest approach (07:17 to 07:24), the Bz_{CSE} sensor is in saturation, and no correlation analysis can be performed. From the first two intervals for the inbound leg (Fig. 8, top panels), we see that enhanced correlation and therefore draping starts at 07:00, increases yet more in the next interval and continues after the tangential discontinuity till the end of the interval (07:16). On the outbound leg, strong correlation is again found from 07:24 to 07:27, which diminishes as the S/C leaves the close neighbourhood of the comet (Fig. 8, bottom panels).

We find that draping is explicit in the interval 07:00 to 07:27 and conclude that the S/C is located in the magnetic pileup region (MPR). Explicit draping ends at 07:27 at a distance of 3.4×10^4 km, which may be interpreted as the outbound crossing of the MPR and MPB.

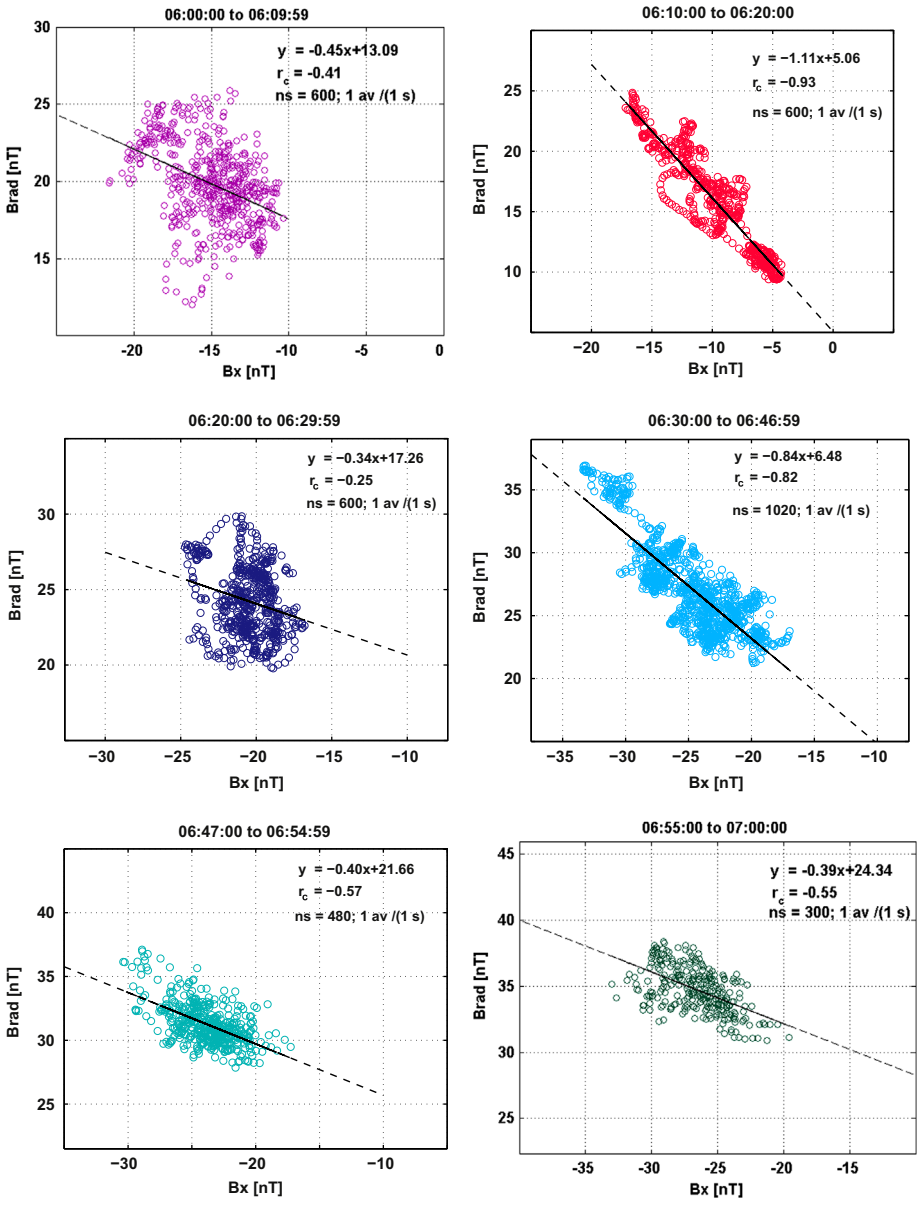

Fig. 6. Correlation between Bx_{IMF} and B_{rad}, for six intervals before closest approach; the color coding refers to the respective time interval in Fig. 5. (For interpretation of the references to color in this figure legend, the reader is referred to the web version of this article.)

3. Discussion

3.1. MPB and MPR

On the inbound leg, after the bow shock crossing at 1.1×10^6 km (at 03:10, not in this data-set), the S/C was located in the cometary magnetosheath; strong fluctuation occurs up to a distance of 3.3×10^5 km (06:10) but is reduced until 1.5×10^5 km (06:47). After that, the variability increases again. Draping is low for the whole interval 06:00 to 07:00.

The magnetic pileup boundary (MPB) as the outer edge of the induced magnetosphere is identified at 06:10 in a distance of 3.5×10^5 km, from the decrease in the fluctuation. It is clear that the restart of turbulence at 06:47 and the reported occurrence of cold cometary ions (06:55) do not coincide with the start of draping at 07:00. At 06:55 and distance 1.2×10^5 km the number density of the cometary ions is not yet high enough, the induced magnetic field effect still too weak to cause significant draping of the field lines. At 07:00 and a closer distance of 9.6×10^4 km, the correlation between the Bx_{IMF} and B_{rad} field component is high, indicating strongly enhanced draping of the field lines. Also the magnetic field strength increases further. The S/C has now entered the magnetic pileup region (MPR) or the real induced magnetosphere, after a gradual transition from the reported start of occurrence of cold cometary ions in 1.2×10^5 km (06:55), down to the fully developed pattern of field draping.

Near closest approach a drop in the field strength was not detected, which means that the S/C did not enter the magnetic cavity. Here, the magnetic field lines follow a plasma which is denser and cooler, due to the prevalence of cold, heavy ions of cometary origin (Gringauz et al., 1986).

On the outbound leg after closest approach, the S/C remained in the induced magnetosphere up to a distance of about 3.4×10^4 km (at 07:27). At later times, the strong correlation between the Bx_{IMF} and B_{rad} field components is not longer existent and the S/C has left the MPB. This is compatible with the occurrence of mirror mode waves after 07:30 (Vaisberg et al., 1989). Due to the asymmetric orbit of the S/C with respect to

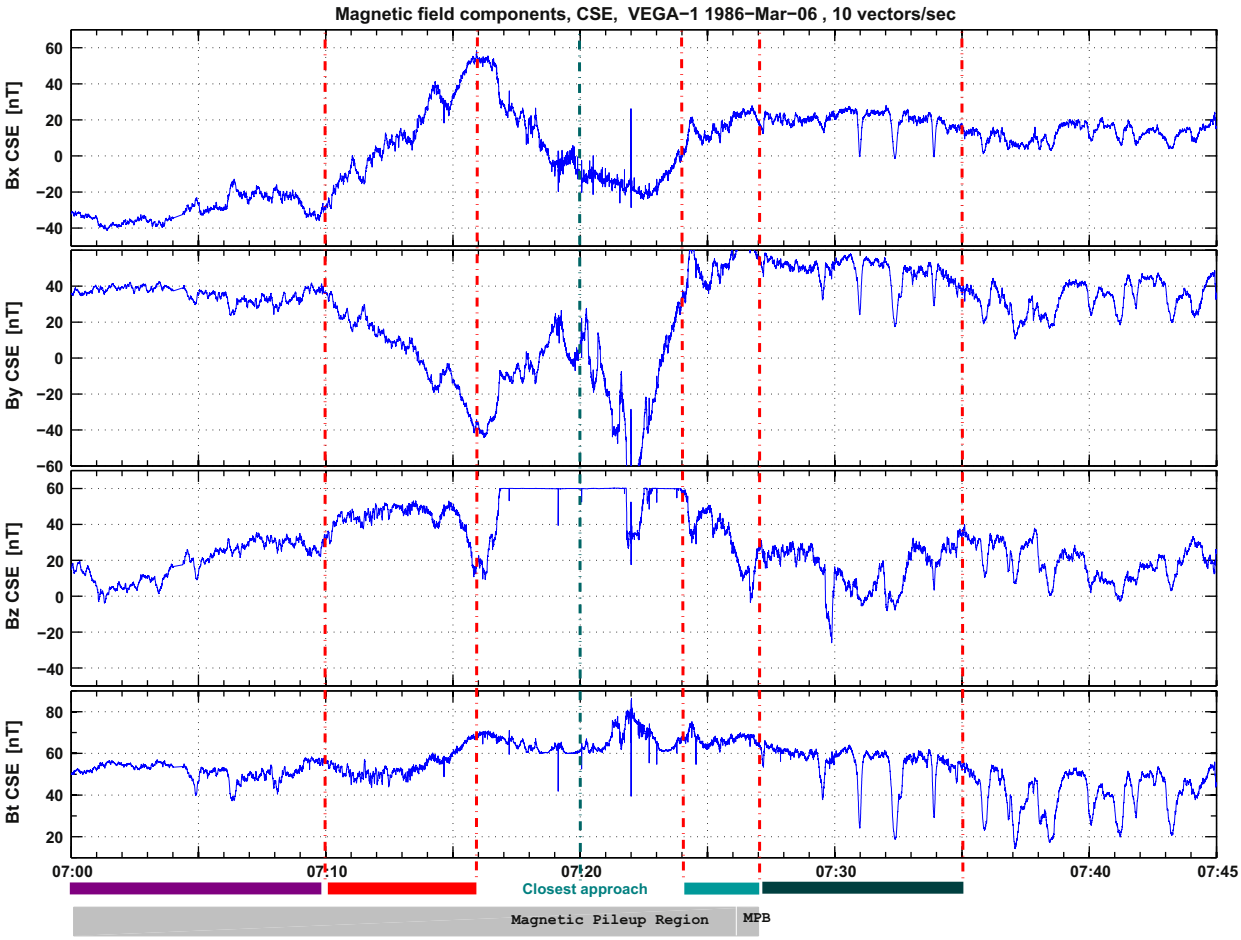

Fig. 7. Magnetic field components and total field in the CSE frame, 1986 Mar 06, 07:00–07:45 around closest approach; each time interval is indicated with a specific color. The sensor for the Bz_{CSE} component was in saturation between 07:16 and 07:24. The grey bar indicates the possible location of the MPR and outbound MPB according to the draping analysis. (For interpretation of the references to color in this figure legend, the reader is referred to the web version of this article.)

the comet, the MPB is crossed in a smaller distance on the outbound leg.

3.2. Waves in or near the MPB

A few strong field fluctuations were observed at 07:04, 07.06 before the closest approach and within the MPB, as well as quasi-periodic strong fluctuations after closest approach between 07:28 and 07:45, out of the MPB and back in the magnetosheath.

The field fluctuations between 07:28 and 07:45 after closest approach were identified as mirror mode (MM) waves, because of their propagation perpendicular to the mean field and ion densities anti-correlated with the magnetic field strength (Vaisberg et al., 1989).

For the field fluctuations before the closest approach and within the MPB, no high resolution ion nor electron data are available, and a decision on the wave-type can be based on the magnetometer data only. Because of the similarity with the fluctuations after closest approach, these waves were also interpreted as mirror mode waves (Russell et al., 1991). However, mirror mode waves are not expected within the MPB, because the ratio of the plasma pressure to the magnetic pressure is low due to the high field strength (low plasma β); at planets, mirror mode waves are only found in the magnetosheath, not within the MPB.

From the Giotto S/C, mirror mode waves were only reported in the magnetosheath. After inbound crossing of the MPB (at 1.35×10^5 km) and in the pileup region, fast mode waves were found, where the oscillations of electron density and magnetic field were in phase (Mazelle et al., 1991; Glassmeier et al., 1993). Such fast mode magnetosonic waves can be generated in a multi-ion plasma, where coherent generation of a velocity difference between the protons and the ions occurs; this is possible after a plasma boundary like the MPB (Sauer et al., 1990).

Since from the Giotto-data, a change of the wave mode was observed at the MPB with fast mode waves inside the MPB, we re-analyse the nature of the waves from Vega-1, in absence of high-resolution ion data for part of the time. A method using only magnetometer data was presented by Lucek et al. (1999a, 1999b) for Equator-S, identifying MM waves as having large strengths DB/B and small angles ($\theta \leq 30^\circ$) between the maximum variance and the magnetic field direction (Price et al., 1986). In addition, the angle between the minimum variance direction and $\boldsymbol{B}$ is expected to be nearly perpendicular (Volwerk et al., 2008).

A minimum variance analysis was performed for the data-interval 06:50 to 07:50 around closest approach, and the angles of the mean field relative to the maximum and minimum variance directions were determined from sliding windows (width = 120 s, shift 6 s). Fig. 9 shows the respective angles, as well as the magnetic field strength. According to the above criteria, the features in the interval marked with blue vertical lines (07:31–07:44) are clearly MM waves: the angle of the mean field with the max. variance direction is small ($\theta \leq 30^\circ$) and the angle with the min. variance direction is nearly perpendicular ($\phi \geq 75^\circ$); the MM waves are compressional and propagate perpendicular to the mean field. This is in agreement with the results from the

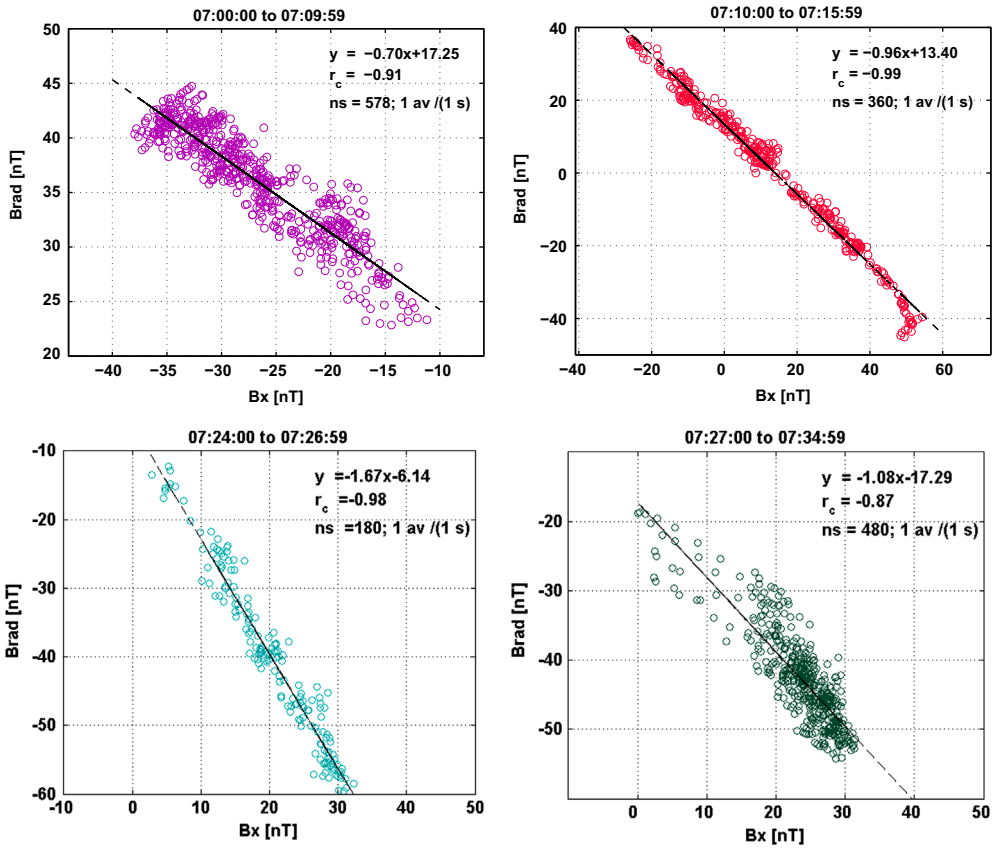

Fig. 8. Correlation between Bx_{IMF} and B_{rad}, for four intervals around closest approach, the color refers to the respective time interval in Fig. 7. For the interval 07:16 to 07:24 no correlation is calculated, because the Bz_{CSE} component was in saturation. (For interpretation of the references to color in this figure legend, the reader is referred to the web version of this article.)

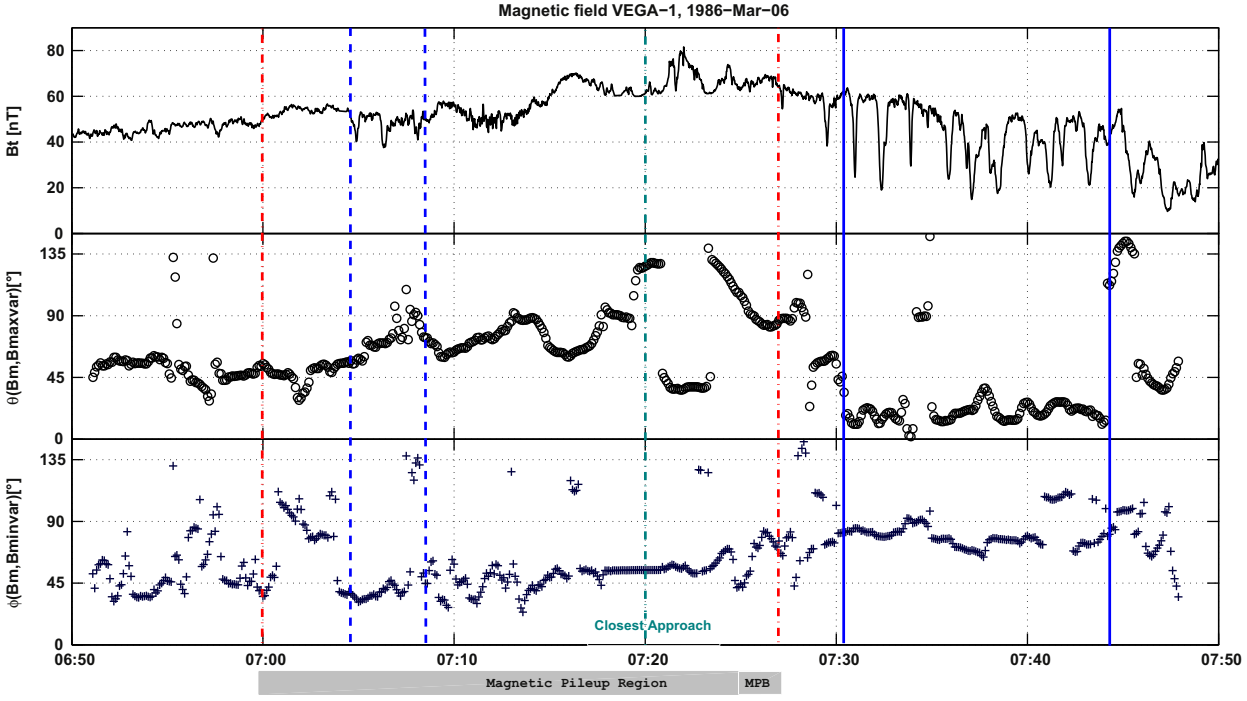

Fig. 9. Wave features in time interval 06:50 to 07:50 near the MPR and MPB. Top panel: magnetic field strength; middle panel: angle θ between mean $\boldsymbol{B}$ and max. variance direction; lower panel: angle ϕ between mean $\boldsymbol{B}$ and min. variance direction. Vertical full lines (blue) indicate the outbound interval with MM waves in the magnetosheath, identified from their correlation with ion density data; dashed lines (blue) indicate the inbound interval within the MPB where different characteristics are found. The red dash-dot lines indicate the location of the MPR and MPB boundaries. (For interpretation of the references to color in this figure legend, the reader is referred to the web version of this article.)

correlation of the magnetic field strength with the ion density data (Vaisberg et al., 1989). However, the features inside the MPR and before closest approach (interval 07:04 to 07:08, marked with blue dashed lines) do not fulfil the criteria for MM waves; their signature in the angles is totally different from the MM waves after closest approach.

We therefore conclude, that the wave structures observed at 07:04, 07.06 and 07:08 within the MPB might not be MM waves. Based on previous work on waves within the MPR (Mazelle et al., 1991) these could be compressive fast-mode magnetosonic waves.

It has to be noted, that although the Vega-1 and Giotto S/C found a similar location of the bow shock, the magnetic pressure in the magnetosheath was completely different during the encounters; this feature might have an impact on the pressure balance at the different plasma boundaries.

4. Conclusion

We have studied the draping characteristics of the magnetic field in the magnetosheath down to closest approach of Comet Halley, from magnetic field data observed by Vega-1. We found that the concept of the different regions magnetic pileup boundary (MPB) and magnetic pileup region (MPR), known for planets with induced magnetosphere, can also well be used to describe/find the induced magnetic boundary for the flyby of Comet Halley by Vega-1. Calculation of the correlation between the field component towards the Sun and the radial component in an aberrated cometocentric frame is very useful to determine if the S/C has entered the MPR and the induced magnetosphere proper.

Due to the much larger dimension of the interaction region and bow shock at comets than at planets, at Comet Halley the MPB appears to be the outer boundary of a wider transition region and magnetic field draping does not start immediately after the MPB was crossed. The increased draping is a clear signal that the induced magnetosphere is entered, but cold cometary ions were already observed just outside of the region of strong draping. So from the magnetometer data, a rather gradual transition from the MPB into the MPR and induced magnetosphere at Comet Halley is found. This is in agreement with the reported bow "wave" instead of a bow shock at this comet, also indicating a gradual transition from unshocked to shocked solar wind.

Previously reported wave features now within the here determined MPR on the inbound trajectory may be identified as compressive fast-mode magnetosonic waves. On the outbound trajectory, waves out of the MPB are confirmed to be mirror mode waves.

For the upcoming encounter of the Rosetta S/C with Comet Churyumov–Gerasimenko, magnetic field and plasma observations may reveal, if the above picture of the fine structure of the MPB and gradual transition into the induced magnetosphere is a more general feature at comets.

Acknowledgments

The authors thank the International Space Science Institute (ISSI, Switzerland) for supporting this work through the working group on Comparative Induced Magnetospheres. MD, MV, CB and NR were also supported by BMWF/ÖAD (Austria) and MINCYT/OEI (Argentina).

References

Alfvèn, H.T., 1957. On the theory of comet tails. Tellus 9.1, 92–96.
Auster, H.U., Apathy, I., Berghofer, G., Remizov, A., Roll, R., Fornacon, K.H., Glassmeier, K.H., Haerendel, G., Hejja, I., Kührt, E., Magnes, W., Moehlmann, D., Motschmann, U., Richter, I., Rosenbauer, H., Russell, C.T., Rustenbach, J., Sauer, K., Schwingenschuh, K., Szemerey, I., Waesch, R., 2007. Romap: Rosetta magnetometer and plasma monitor. Space Sci. Rev. 128, 221–240, http://dx.doi.org/10.1007/s11214-006-9033-x.
Bertucci, C., Duru, F., Edberg, N., Fraenz, M., Martinecz, C., Szegö, K., Vaisberg, O., 2011. The induced magnetospheres of Mars, Venus, and Titan. Space Sci. Rev. 162, 113–171, http://dx.doi.org/10.1007/s11214-011-9845-1.
Bertucci, C., Mazelle, C., Crider, D.H., Vignes, D., Acun~a, M.H., Mitchell, D.L., Lin, R.P., Connerney, J.E.P., Rème, H., Cloutier, P.A., Ness, N.F., Winterhalter, D., 2003a. Magnetic field draping enhancement at the Martian magnetic pileup boundary from Mars global surveyor observations. Geophys. Res. Lett. 30, 1099, http://dx.doi.org/10.1029/2002GL015713.
Bertucci, C., Mazelle, C., Slavin, J.A., Russell, C.T., Acun~a, M.H., 2003b. Magnetic field draping enhancement at Venus: evidence for a magnetic pileup boundary. Geophys. Res. Lett. 30, 1876, http://dx.doi.org/10.1029/2003GL017271.
Glassmeier, K.-H., Boenhardt, H., Koschny, D., Kührt, E., Richter, I., 2007a. The ROSETTA mission: flying towards the origin of the solar system. Space Sci. Rev. 128, 1–21, http://dx.doi.org/10.1007/s11214-006-9140-8.
Glassmeier, K.-H., Motschmann, U., Mazelle, C., Neubauer, F.M., Sauer, K., Fuselier, S.A., Acuña, M.H., 1993. Mirror modes and fast magnetoacoustic waves near the magnetic pileup boundary of comet P/Halley. J. Geophys. Res. 98 (A12), 20955–20964.
Glassmeier, K.-H., Richter, I., Diedrich, A., Mussmann, G., Auster, U., Motschmann, U., Balogh, A., Carr, C., Cupido, E., Coates, A., Rother, M., Schwingenschuh, K., Szegö, K., Tsurutani, B., 2007b. RPC-MAG the fluxgate magnetometer in the ROSETTA plasma consortium. Space Sci. Rev. 128, 649–670, http://dx.doi.org/10.1007/s11214-006-9114-x.
Gringauz, et al., 1986. First in situ plasma and neutral gas measurements at comet Halley. Nature 321, 282.
Israelevich, P.L., et al., 1994. The induced magnetosphere of comet Halley: interplanetary magnetic field during Giotto encounter. J. Geophys. Res. 99 (A4), 6575–6583.
Lucek, E.A., Dunlop, M.W., Balogh, A., Cargill, P., Baumjohann, W., Georgescu, E., Haerendel, G., Fornac, K.-H., 1999a. Mirror mode structures observed in the dawn-side magnetosheath by Equator-S. Geophys. Res. Lett. 26, 2159–2162.
Lucek, E.A., Dunlop, M.W., Balogh, A., Cargill, P., Baumjohann, W., Georgescu, E., Haerendel, G., Fornac, K.-H., 1999b. Identification of magnetosheath mirror modes in Equator-S magnetic field data. Ann. Geophys. 17, 1560–1573.
Mazelle, C., Belmont, G., Glassmeier, K.H., Le Quéau, D., Rème, H., 1991. Ultra low frequency waves at the magnetic pile-up boundary of comet P/Halley. Adv. Space Res. 11, 73.
Neubauer, F.M., Glassmeier, K.H., Pohl, M., Raeder, J., Acuna, M.H., Burlaga, L.F., Ness, N.F., Musmann, G., Mariani, F., Wallis, M.K., Ungstrup, E., Schmidt, H.U., 1986. First results from the Giotto magnetometer experiment at comet Halley. Nature 321, 352.
Neubauer, F.M., 1987. Giotto magnetic-field results on the boundaries of the pile-up region and the magnetic cavity. Astron. Astrophys. 187, 73–79.
Price, C.P., Swift, D.W., Lee, L.-C., 1986. Numerical simulation of nonoscillatory mirror waves at the Earth's magnetosheath. J. Geophys. Res. 91, 101–112.
Reinhard, R., 1986. The Giotto encounter with comet Halley 1986. Nature 321, 313.
Rème, H., Mazelle, C., d'Uston, C., Korth, A., Lin, R.P., Chaizy, P., 1994. There is no "cometopause" at comet Halley. J. Geophys. Res. 99 (A2), 2301–2308.
Riedler, W., Schwingenschuh, K., Yeroshenko, Y.e., Styashkin, V.A., Russell, C.T., 1986. Magnetic field observations in comet Halley's coma. Nature 321, 288.
Russell, C.T., Le, G., Schwingenschuh, K., Riedler, W., 1991. Mirror mode waves at comet Halley, in "Cometary Plasma Processes". Geophysical Monograph, 61. AGU.
Sauer, K., Motschmann, U., Roatsch, Th., 1990. Plasma boundaries at comet Halley. Ann. Geophys. 8, 243–250.
Schwingenschuh, K., Riedler, W., Schelch, G., Yeroshenko, Y.e., Styashkin, V.A., Luhmann, J.G., Russell, C.T., Fedder, J.A., 1986. Cometary boundaries: Vega observations at Halley. Adv. Space Res. 6, 217.
Vaisberg, O.L., Russell, C.T., Luhmann, J.G., Schwingenschuh, K., 1989. Small scale irregularities in comet Halley's plasma mantle: an attempt at self-consistent analysis of plasma and magnetic field data. Geophys. Res. Lett. 16, 5–9.
Volwerk, M., Zhang, T.L., Delva, M., Vörös, Z., Baumjohann, W., Glassmeier, K.-H., 2008. First identification of mirror mode waves in Venus' magnetosheath. Geophys. Res. Lett. 35, L12204, http://dx.doi.org/10.1029/2008GL033621.
von Rosenvinge, T.T., Brandt, J.C., Farquhar, R.W., 1986. The international cometary explorer mission to comet Giacobini–Zinner. Science 232, 353 (doi:10.1126/science.232.4748.353).